

Relativistic accretion and burdened primordial black holes

Suvashis Maity^{1*},

¹ Department of Physics, Indian Institute of Science Education and Research, Pune 411008, India

E-mail: *saamaity@gmail.com

Abstract. We examine the joint effects of relativistic accretion and memory burdened evaporation on the evolution of primordial black holes (PBHs). The memory burden effect, which delays the evaporation by inducing a backreaction and making the evaporation rate scale as an inverse power law of the PBH entropy, opens up a new window that allows PBHs with $M \lesssim 10^{15}$ g to survive until the present epoch. Meanwhile, accretion increases the mass of PBHs, thereby enhancing their chances of survival for a given initial mass. We consider two main scenarios: one where PBHs evaporate completely before big bang nucleosynthesis, and another where PBHs persist until today. In the case of evaporation, we analyze the emission of dark matter (DM) and dark radiation (DR) during the process of evaporation. Conversely, in the other case, the surviving PBHs themselves can contribute as DM. We further investigate how relativistic and non-relativistic accretion, together with memory burdened evaporation, impact the parameter space of the emitted DM, the abundance of stable PBHs as DM, and the contribution of DR to the effective number of relativistic degrees of freedom, ΔN_{eff} .

Contents

1	Introduction	1
2	Evolution of the mass of PBHs	3
2.1	Accretion of PBHs	3
2.2	Evaporation of PBHs	4
2.3	Total mass evolution of PBHs:	5
3	Production of dark matter from evaporation of PBHs	8
3.1	The case with $\beta > \beta_{\text{cr}}$	10
3.2	The case with $\beta < \beta_{\text{cr}}$	11
3.3	Constraints from warm dark matter	13
4	Dark matter from stable PBHs	14
5	Dark radiation from the evaporation of PBHs	16
6	Conclusions	17

1 Introduction

Primordial black holes (PBHs) have attracted widespread interest over the past few decades [1]. They are thought to form from the collapse of overdense regions in the early universe. Due to their cold and non-interacting nature, PBHs are also considered a compelling candidate for dark matter (DM) [1–11]. Recent detections of binary black hole mergers by the LIGO-Virgo collaboration have further revived interest in PBHs, as they could potentially contribute to the observed merger rate [12–17]. Moreover, there have been numerous recent efforts to constrain the fraction of DM that can be in the form of PBHs by analyzing scalar-induced secondary gravitational waves (GWs) probed by pulsar timing arrays [18–24].

PBHs are also metastable objects that can evaporate over time, emitting various particles through the process of evaporation [25, 26]. During evaporation, PBHs can emit standard model (SM) particles [27, 28] (which may potentially reheat the universe), contribute to the relic abundance of DM [29–32], generate dark radiation (DR) [33–35] or produce high-frequency GWs [36–40], thereby influencing several cosmological observables. In a semiclassical framework, PBHs undergo Hawking evaporation, leading to stringent constraints: PBHs with masses $M < 10^{15}$ g would have largely evaporated by today, while those with masses $M < 10^9$ g would have evaporated before about one second, thus impacting BBN and being constrained by the abundance of light elements.

Recent studies have revealed that quantum effects play a pivotal role in the evaporation of PBHs at later stages. As a PBH loses mass via Hawking radiation, its associated entropy decreases. Since black hole entropy encodes the number of microstates, this loss leads to a reduction in the information-storing capacity of the system. However, if evaporation of PBHs is unitary, as demanded by quantum mechanics, this loss of information must be accounted for. The resulting backreaction on the process of evaporation, arising from the burden of retaining information is known as the memory burden effect [41–44]. This effect can significantly slow

down or even stabilize the evaporation, effectively allowing PBHs to persist longer than predicted by standard Hawking evaporation.

One of the most striking consequences is that PBHs with masses below 10^{15} g, which would otherwise have evaporated completely by the present epoch, may still survive. This opens up a new mass window in the allowed parameter space for the fraction of DM contributed by PBHs, f_{PBH} [45–48]. Moreover, the memory burden effect has been shown to impact a variety of cosmological observables and theoretical processes. These include potential signatures in the stochastic GW background [35, 49–55], implications for DM [47, 53, 56–61], baryogenesis mechanisms such as leptogenesis [62–64], and other phenomena that remain active areas of investigation [65–74].

Other than evaporation, PBHs can also accrete matter from their surroundings, potentially increasing their mass. For PBHs modeled as Newtonian point masses embedded in an infinite homogeneous gas cloud, Bondi [75] (for related discussions, see [76–87]) first analysed the spherically symmetric, steady-state accretion flow. However, when the velocity of the infalling matter approaches relativistic speeds or the background temperature becomes high, the accretion dynamics require relativistic corrections to the classical Bondi-Hoyle formalism [88, 89]. In such a regime, the rate of accretion becomes highly sensitive to the mass of PBHs, the energy density of the surrounding medium, and its equation of state (EoS). Recent studies have shown that relativistic accretion can substantially enhance the growth of the mass of PBHs, particularly when they form during early, dense phases [89]. These effects can modify the mass of PBHs, affect their survival probability, and lead to important implications for cosmological constraints.

In this work, we have investigated the relativistic accretion of PBHs with a lower mass that would otherwise have completely evaporated before the onset of BBN via Hawking radiation. We examine how relativistic accretion influences the process of evaporation, particularly when combined with the effects of memory burden. The accretion can further prolong the lifetime of such PBHs, potentially allowing them to survive past the epoch of BBN. We also study the production of DM from the evaporation of PBHs and examine how both relativistic accretion and memory burden modify the allowed parameter space for DM emitted. Furthermore, for PBHs that may still exist today due to memory burden effects, we apply existing constraints on f_{PBH} in the newly opened mass window ($< 10^{15}$ g) [45–48]. Using these, we derive bounds on the initial abundance of PBHs and demonstrate how these constraints differ from scenarios that neglect accretion. Further, we consider the emission of DR from the evaporation of PBHs and discuss the contribution of DR to the ΔN_{eff} , especially in the light of relativistic accretion and burdened evaporation.

This paper is organised as follows. In Sec. 2, we discuss the evolution of the mass of PBHs, taking into account both relativistic accretion and burdened evaporation. In Sec. 3, we examine the DM produced from the evaporation of PBHs and explore how accretion and evaporation affect the parameter space of the emitted DM. Further, in Sec. 4, we discuss the stable PBHs in the new mass window arising due to the memory burden, and analyse the impact of accretion on this scenario. In Sec. 5, we investigate the contribution to ΔN_{eff} from DR generated through evaporation. Finally, in Sec. 6, we conclude with a brief summary.

We shall now make a few clarifying remarks on the conventions and notations that we shall adopt in this work. We shall work with natural units such that $\hbar = c = 1$, and the reduced Planck mass is $M_{\text{Pl}} = (8\pi G)^{-1/2} \simeq 2.4 \times 10^{18}$ GeV. The signature of the metric is followed $(-, +, +, +)$ and the background is spatially flat Friedmann-Lemaître-Robertson-Walker (FLRW). An overdot and an overprime shall denote differentiation with respect to the

cosmic time t and the conformal time η , respectively. Derivatives with respect to any other quantity will be denoted as subscript by the quantity.

2 Evolution of the mass of PBHs

We begin by discussing the evolution of the mass of a PBH under the combined effects of accretion and evaporation. PBHs are assumed to form from the collapse of overdense regions in the early universe, with the mass at the time of formation related to the Hubble parameter at that epoch by $M_{\text{in}} = 4\pi\gamma M_{\text{Pl}}^2 H_{\text{in}}^{-1}$, where $\gamma = w^{3/2}$ is the collapse efficiency, which quantifies the fraction of the mass enclosed within the Hubble radius that collapses to form PBHs. For a background with a general EoS w , the Hubble parameter evolves with cosmic time as $H = 2/[3(1+w)t]$. Substituting this expression into the equation for M_{in} , we obtain the relation between the time of the formation of PBHs t_{in} and the initial mass of PBHs to be

$$t_{\text{in}} = \frac{M_{\text{in}}}{6\pi\gamma(1+w)M_{\text{Pl}}^2}. \quad (2.1)$$

Other than the mass, two important quantities associated with PBHs are their temperature T_{BH} and entropy S , both of which are functions of the PBH mass as

$$T_{\text{BH}} = \frac{M_{\text{Pl}}^2}{M}, \quad S = \frac{1}{2} \left(\frac{M}{M_{\text{Pl}}} \right)^2. \quad (2.2)$$

The above relations in Eq. (2.2), indicate that a PBH with lower mass will have higher energy but lower entropy. The energy density of PBHs, ρ_{BH} is related to the number density n_{BH} as $\rho_{\text{BH}} = n_{\text{BH}} \times M$. While the cosmic expansion causes the number density to dilute as $n_{\text{BH}} \sim a^{-3}$, the mass of individual PBHs is not conserved, as it evolves due to the competing effects of accretion and evaporation. In what follows, we will discuss in detail how these two processes influence the evolution of mass over time.

2.1 Accretion of PBHs

The rate of change of mass of PBHs due to the accretion is given by [88, 89]

$$\frac{dM}{dt} = \frac{\lambda_c}{16\pi} \frac{M^2}{M_{\text{Pl}}^4} \rho_{\infty}, \quad (2.3)$$

where ρ_{∞} is the energy density of the background. The quantity λ_c is given by $\lambda_c^{\text{R}} = (1/4)w^{-3/2}(1+3w)^{(1+3w)/2w}$ for a relativistic fluid, whereas for a non-relativistic fluid $\lambda_c^{\text{NR}} = (1/4)(e/w)^{3/2}$ [90]. For a background with EoS w , the energy density in terms of the cosmic time is given as $\rho = 3M_{\text{Pl}}^2 H^2 = 4M_{\text{Pl}}^2/[3(1+w)^2 t^2]$. Clearly $\lambda_c = 0$ indicates that there is no accretion of matter. Using this behaviour of ρ_{∞} , it is straightforward to integrate Eq. (2.3) to find the mass of PBHs at any time as [89]

$$M(t) = M_{\text{in}} \left[1 - \frac{\lambda_c \gamma}{2(1+w)} \frac{(3/2)(1+w)H_{\text{in}}(t-t_{\text{in}})}{(3/2)(1+w)H_{\text{in}}(t-t_{\text{in}}) + 1} \right]^{-1}. \quad (2.4)$$

A common intuition is that as a PBH survives longer, it continues to grow by accreting surrounding matter or radiation. To understand this quantitatively, let us analyze the

behaviour described by Eq. (2.4). At early times, accretion is efficient due to high density of the background, but as the universe expands and ρ_∞ falls, the rate of accretion decreases. Eventually, at a later time ($t \gg t_{\text{in}}$), the accretion saturates when the rate of fractional mass growth becomes equal to the Hubble parameter, i.e., $\dot{M}/M = H$, and the mass becomes

$$M_{\text{acc}} \simeq M_{\text{in}} \left(1 - \frac{\lambda_c \gamma}{2(1+w)} \right)^{-1}. \quad (2.5)$$

Equation (2.5) shows that in a radiation-dominated background ($w = 1/3$), the total mass gain from relativistic accretion can be estimated as $M_{\text{acc}}/M_{\text{in}} \approx 4$. For higher values of the w , this ratio increases, and can reach $\mathcal{O}(100)$ for sufficiently stiff backgrounds. Notably, in the limit of a stiff fluid ($w = 1$), the expression formally yields $M_{\text{acc}}/M_{\text{in}} \rightarrow \infty$. This apparent divergence arises because accretion requires the black hole to pull matter in faster than the fluid can respond via pressure. In the case of a stiff fluid, pressure disturbances propagate at the speed of light, making the fluid extremely resistant to compression or inward flow. As a result, no steady-state, transonic accretion solution exists, and the standard formalism becomes ill-defined in this limit. Hence, in this work, we focus on two representative background EoS values: $w = 1/3$ (radiation domination), and a stiffer case of $w = 2/3$, as illustrative toy models.

2.2 Evaporation of PBHs

The rate of change of the mass of PBHs due to Hawking evaporation, including the effects of quantum memory burden, is given by [25, 45, 46]

$$\frac{dM}{dt} = -\epsilon \frac{M_{\text{Pl}}^4}{M^2} S^{-\kappa \Theta(t-t_q)}, \quad (2.6)$$

where the negative sign reflects the loss of mass due to evaporation. The parameter ϵ is the greybody factor [30, 91–93], which encodes the frequency-dependent transmission probabilities for particles emitted by the PBH evaporation. In the geometric optics limit, it is approximately given by $\epsilon \simeq (27/4) g(T_{\text{BH}}) \pi / 480$, where $g(T_{\text{BH}})$ is the effective number of relativistic degrees of freedom at the black hole temperature, T_{BH} , and we have $g(T_{\text{BH}}) \simeq 106.75$. The factor $S^{-\kappa}$ accounts for the quantum memory burden, which suppresses the evaporation rate once a significant portion of the PBH's mass has been radiated away.

Initially, PBHs evaporate through the standard semiclassical Hawking radiation. However, once the mass of PBHs reduces to a fraction q of its initial mass M_{in} , memory burden effects become significant, modifying the rate of evaporation and potentially stabilizing the PBH remnant [41–44]. The time at which memory burden starts to dominate is given by $t_q = (1 - q^3)t_{\text{ev}}^0$, where $t_{\text{ev}}^0 \simeq M_{\text{in}}^3 / (3\epsilon M_{\text{Pl}}^4)$ is the time of evaporation of the PBH in a semi-classical process. The final time of evaporation due to the memory burden is given by $t_{\text{ev}}^\kappa = [2^\kappa (3 + 2\kappa) M_{\text{Pl}}]^{-1} (q M_{\text{in}} / M_{\text{Pl}})^{3+2\kappa}$ [45, 47]. The mass of the PBHs at any time is now given by

$$M(t) = \begin{cases} M_{\text{in}} \left[1 - \frac{t-t_{\text{in}}}{t_{\text{ev}}^0} \right]^{1/3} & \text{for } t < t_q, \\ q M_{\text{in}} \left[1 - \frac{t-t_q}{t_{\text{ev}}^\kappa} \right]^{1/(3+2\kappa)} & \text{for } t > t_q. \end{cases} \quad (2.7)$$

We note that the exact value of the memory burden parameter κ is currently undetermined, and in this work, we treat it as a free phenomenological parameter. The limiting case

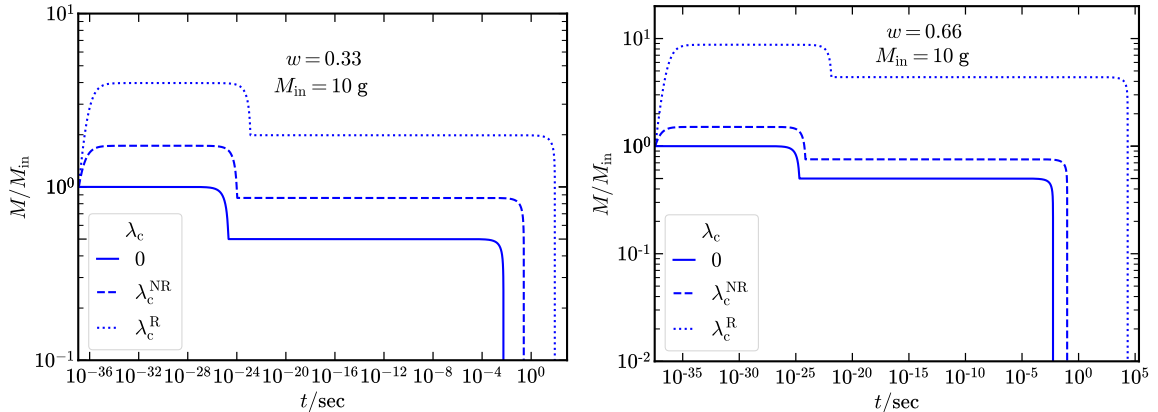


Figure 1. The evolution of the mass of PBHs under the combined effects of accretion and burdened evaporation is shown for two different background equations of state: $w = 1/3$ (left panel) and $w = 2/3$ (right panel). In each plot, the solid line denotes the evolution of the mass of PBHs without accretion, i.e., purely due to evaporation with memory burden effects. We have fixed the parameter values to $\kappa = 2$, $q = 1/2$. The dashed line represents the evolution when PBHs accrete from a non-relativistic fluid background, while the dotted line corresponds to accretion from a relativistic fluid.

$\kappa = 0$, $q = 1$ corresponds to standard Hawking evaporation without any memory burden effects. In principle, the parameter q can take values in the range $0 < q < 1$. However, following previous discussions in the literature, we adopt the representative value $q = 1/2$, for which the memory burden is expected to become relevant [45, 46].

2.3 Total mass evolution of PBHs:

So far, we have discussed two key physical processes that govern the evolution of the mass of PBHs after their formation: accretion, through which PBHs gain mass by drawing in surrounding matter or radiation, and evaporation, by which they lose mass through the emission of particles. To accurately capture the time evolution of the mass of PBHs, it is essential to incorporate both effects simultaneously. The total rate of change of the PBH mass is therefore given by the combined equation

$$\frac{dM}{dt} = \left. \frac{dM}{dt} \right|_{\text{accretion}} + \left. \frac{dM}{dt} \right|_{\text{evaporation}}. \quad (2.8)$$

At the initial stage of PBH evolution, accretion dominates over evaporation due to the high background energy density. During this phase, PBHs rapidly gain mass until reaching a saturation value M_{acc} , beyond which accretion becomes inefficient and evaporation effects begin to take over. The timescale for this accretion-driven growth, denoted by the interval $[t_{\text{in}}, t_{\text{acc}}]$, is typically much shorter than the subsequent timescale of evaporation $[t_{\text{acc}}, t_{\text{ev}}]$. Given this clear separation of timescales, the evolution of the PBH mass can be well approximated analytically by treating M_{acc} as the effective initial mass for the evaporation-dominated phase.

The complete evolution of the mass of a PBH can now be expressed as

$$M(t) = \begin{cases} M_{\text{in}} \left[1 - \frac{\lambda_c \gamma}{2(1+w)} \frac{(3/2)(1+w)H_{\text{in}}(t-t_{\text{in}})}{(3/2)(1+w)H_{\text{in}}(t-t_{\text{in}})+1} \right]^{-1} & \text{for } t_{\text{in}} < t < t_{\text{acc}}, \\ M_{\text{acc}} \left[1 - \frac{t-t_{\text{acc}}}{t_{\text{ev}}^0} \right]^{1/3} & \text{for } t_{\text{acc}} < t < t_{\text{q}}, \\ qM_{\text{acc}} \left[1 - \frac{t-t_{\text{q}}}{t_{\text{ev}}^\kappa} \right]^{1/(3+2\kappa)} & \text{for } t_{\text{q}} < t < t_{\text{ev}}, \end{cases} \quad (2.9)$$

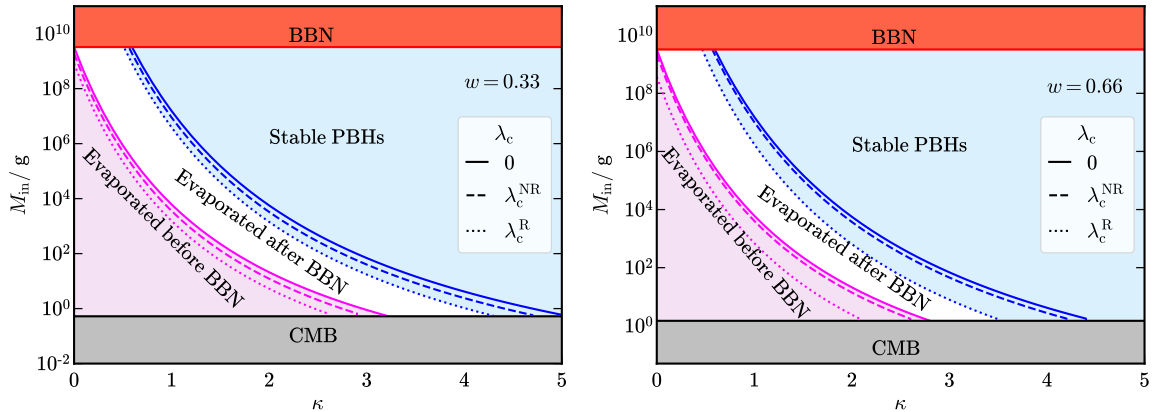


Figure 2. The allowed range of the initial PBH mass M_{in} as a function of the memory burden parameter κ is shown for two background equations of state: $w = 1/3$ (left panel) and $w = 2/3$ (right panel). The region is bounded from above and below by two key constraints. The grey shaded region at the bottom corresponds to the minimum initial PBH mass allowed by the maximum energy scale of inflation, consistent with the current observational upper bound on the tensor-to-scalar ratio $r = 0.036$. The red shaded region indicates values of M_{in} for which the semiclassical evaporation completes after the onset of BBN. The magenta curves show the upper bound on M_{in} for which PBHs evaporate completely before BBN, while the blue curves mark the lower bound for which PBHs can survive until the present epoch. The solid, dashed, and dotted curves correspond to scenarios with $\lambda_c = 0$, λ_c^{NR} , and λ_c^{R} , respectively.

with the modified expressions of time to be

$$t_{\text{ev}}^0 \simeq \frac{M_{\text{in}}^3}{3\epsilon M_{\text{Pl}}^4} \left(1 - \frac{\lambda_c \gamma}{2(1+w)}\right)^{-3} \quad (2.10)$$

$$t_q \simeq \frac{(1-q^3)M_{\text{in}}^3}{3\epsilon M_{\text{Pl}}^4} \left(1 - \frac{\lambda_c \gamma}{2(1+w)}\right)^{-3} \quad (2.11)$$

$$t_{\text{ev}}^\kappa \simeq \frac{1}{2^\kappa (3+2\kappa)\epsilon M_{\text{Pl}}} \left(\frac{qM_{\text{in}}}{M_{\text{Pl}}}\right)^{(3+2\kappa)} \left(1 - \frac{\lambda_c \gamma}{2(1+w)}\right)^{-(3+2\kappa)}. \quad (2.12)$$

Clearly, the expression for the time of evaporation, t_{ev}^κ , given in Eq. (2.12), represents the most general case. Here, setting $\lambda_c = 0$ corresponds to the scenario without accretion, while λ_c^{NR} and λ_c^{R} denote the cases with non-relativistic and relativistic accretion, respectively. Furthermore, the choice $\kappa = 0$ and $q = 1$ recovers the standard case of Hawking evaporation. In Fig. 1, we illustrate the evolution of the mass of PBHs over time. We have chosen the initial mass of the PBH to be 10 g, and the two panels correspond to different background EoS, namely $w = 1/3$ and $w = 2/3$, respectively. The solid, dashed, and dotted lines represent the evolution of the PBH mass in the absence of accretion ($\lambda_c = 0$), with non-relativistic accretion (λ_c^{NR}), and with relativistic accretion (λ_c^{R}), respectively. We have fixed the parameters characterising the memory burden to $\kappa = 2$ and $q = 1/2$. It can be seen that the initial mass gain, $M_{\text{acc}}/M_{\text{in}}$, due to relativistic accretion can reach ~ 4 for a background with $w = 1/3$, and can be as large as ~ 10 for $w = 2/3$. The increase in mass due to accretion consequently extends the lifetime of the PBHs, with relativistic accretion leading to an enhancement of the lifetime by several orders of magnitude.

In this work, we focus on two scenarios: one in which the PBH completely evaporates before the onset of BBN, and another in which the PBH survives until the present epoch. By taking into account both accretion and evaporation, the former case imposes a constraint on the initial mass of the PBH, for which the PBH would evaporate entirely before BBN to be

$$M_{\text{in}}^{\text{BBN}} \leq \frac{M_{\text{Pl}}}{q} \left(1 - \frac{\lambda_c \gamma}{2(1+w)} \right) (2^\kappa (3 + 2\kappa) \epsilon t_{\text{BBN}} M_{\text{Pl}})^{1/(3+2\kappa)}. \quad (2.13)$$

From the relation in Eq. (2.13), we see that for evaporation purely via Hawking radiation, the maximum initial mass of PBHs that would evaporate before BBN is approximately $\sim 1.6 \times 10^9$ g in the absence of accretion. This value decreases to $\sim 9.4 \times 10^8$ g and $\sim 4 \times 10^8$ g for non-relativistic and relativistic accretion, respectively, in a radiation-dominated background. For the scenario with a memory burden characterized by parameters $\kappa = 2$ and $q = 1/2$, the maximum allowed initial mass reduces significantly to ~ 21 g, 12 g, and 5 g for $\lambda_c = 0$, λ_c^{NR} , and λ_c^{R} , respectively. Moreover, a different background EoS affects these constraints in the presence of accretion; for instance, with $w = 2/3$, the maximum allowed mass for relativistic accretion further decreases to ~ 2.5 g. In a similar fashion, the minimum mass of a PBH to survive the present epoch is given by

$$M_{\text{in}}^0 \geq \frac{M_{\text{Pl}}}{q} \left(1 - \frac{\lambda_c \gamma}{2(1+w)} \right) (2^\kappa (3 + 2\kappa) \epsilon t_0 M_{\text{Pl}})^{1/(3+2\kappa)}. \quad (2.14)$$

We know that for standard Hawking evaporation without accretion, the minimum mass of PBHs that can survive until today is approximately 10^{15} g. When including the effects of a memory burden with parameters $\kappa = 2$ and $q = 1/2$, this minimum mass shifts significantly, becoming ~ 5600 g, 3200 g, and 1400 g for the cases $\lambda_c = 0$, λ_c^{NR} , and λ_c^{R} , respectively. Moreover, for a background EoS with $w = 2/3$ and relativistic accretion, the minimum mass required for PBHs to survive until the present epoch further decreases to ~ 640 g. In Fig. 2, we illustrate the various constraints on the initial mass of PBHs as a function of the memory burden parameter κ . We consider two values of the background EoS: $w = 1/3$, shown in the left panel, and $w = 2/3$, shown in the right panel. In each plot, the grey shaded regions correspond to the minimum allowed initial mass of PBHs, set by the highest permissible energy scale of inflation inferred from the tensor-to-scalar ratio $r = 0.036$ [94]. The red shaded regions indicate the upper limit on the initial mass above which Hawking evaporation would occur only after BBN, while the magenta lines mark the maximum initial mass for which PBHs would completely evaporate before BBN. In contrast, the blue lines denote the minimum initial mass required for PBHs to survive until the present epoch. The solid, dashed, and dotted lines correspond to the cases with $\lambda_c = 0$, λ_c^{NR} , and λ_c^{R} , respectively. We observe that the constraints arising from relativistic accretion differ significantly from the other cases, with the disparity becoming more pronounced for a stiffer background EoS.

Let us now discuss the possibility that the energy density of PBHs dominates over the energy density of the background before the PBHs evaporate. As the universe expands, the energy densities evolve with the scale factor a as

$$\rho_{\text{BH}} = \rho_{\text{BH}}^{\text{in}} \left(\frac{a_{\text{in}}}{a} \right)^3, \quad \rho_w = \rho_w^{\text{in}} \left(\frac{a_{\text{in}}}{a} \right)^{3(1+w)}, \quad (2.15)$$

where the sub/superscript ‘in’ denotes the quantities at the time of the formation of PBHs. For $w > 0$, the energy density of PBHs redshifts more slowly than the energy density of the

background, implying that even a subdominant initial PBH population could eventually come to dominate the total energy density of the universe before evaporation. We further know that the scale factor behaves with the cosmic time as $a \propto t^{2/[3(1+w)]}$. Using this, we get the time when the energy density of PBHs starts dominating the background energy density as

$$t_{\text{BH}} = t_{\text{in}}(q\beta)^{-(1+w)/(2w)}. \quad (2.16)$$

Moreover, for the PBH domination to take place, the time of the domination needs to be before the time of the evaporation of PBHs, $t_{\text{BH}} \leq t_{\text{ev}}^\kappa$. These conditions lead to the critical value of the initial abundance of PBHs, β , above which there will be PBH domination. The critical value of β is given by

$$\beta_{\text{cr}} = \frac{1}{q} \left(\frac{t_{\text{in}}}{t_{\text{ev}}^\kappa} \right)^{\frac{2w}{1+w}} = \frac{1}{q} \left[\frac{2^\kappa(3+2\kappa)\epsilon}{6\pi\gamma(1+w)q} \left(\frac{M_{\text{Pl}}}{qM_{\text{in}}} \right)^{2(1+\kappa)} \right]^{\frac{2w}{1+w}} \left(1 - \frac{\lambda_c\gamma}{2(1+w)} \right)^{\frac{2w(3+2\kappa)}{1+w}}. \quad (2.17)$$

Again, we get for $\kappa = 2$, $q = 1/2$ and $w = 1/3$,

$$\beta_{\text{cr}}^{\lambda_c=0} = \frac{9.67 \times 10^{-15}}{M_{\text{in}}^3}, \quad \beta_{\text{cr}}^{\lambda_c^{\text{NR}}} = \frac{1.5 \times 10^{-15}}{M_{\text{in}}^3}, \quad \beta_{\text{cr}}^{\lambda_c^{\text{R}}} = \frac{7.5 \times 10^{-17}}{M_{\text{in}}^3},$$

whereas for $w = 2/3$

$$\beta_{\text{cr}}^{\lambda_c=0} = \frac{9.1 \times 10^{-24}}{M_{\text{in}}^{4.8}}, \quad \beta_{\text{cr}}^{\lambda_c^{\text{NR}}} = \frac{9.1 \times 10^{-25}}{M_{\text{in}}^{4.8}}, \quad \beta_{\text{cr}}^{\lambda_c^{\text{R}}} = \frac{4.2 \times 10^{-29}}{M_{\text{in}}^{4.8}}.$$

We shall clarify that, in deriving the expression for β_{cr} , we have assumed the possibility of PBH domination, wherein the universe undergoes a sequence of phases: w -domination \rightarrow PBH domination \rightarrow radiation domination. A more intricate scenario can arise if the inflaton is strongly coupled to SM particles and decays before PBH domination, leading to an intermediate phase of radiation domination prior to PBH domination. In such a case, the subsequent evaporation of PBHs would result in a secondary phase of reheating. In this work, however, we assume a sufficiently small coupling of the inflaton to radiation to avoid these complications and to ensure the simpler sequence of cosmological eras considered.

3 Production of dark matter from evaporation of PBHs

In this section, we discuss the production of DM from the evaporation of PBHs. We specifically restrict our analysis to the mass range of PBHs that ensures they would have evaporated completely before the onset of BBN. We begin by calculating the number of DM particles produced from the evaporation of a single PBH. It is important to note that both the mass and spin of a black hole significantly affect the production rate of particles generated during its evaporation. The emission spectra and greybody factors depend sensitively on the spin of the emitted species as well as the angular momentum of the black hole itself. However, for simplicity, in this work we restrict our analysis to the case of non-rotating, spin-zero Schwarzschild black holes. Under this assumption, the emission rate of a particle species j with mass m_j and internal degrees of freedom g_j , per unit time and per unit energy interval, is given by [27, 47]

$$\frac{d^2 N_j}{dE dt} = \frac{27}{4} \frac{g_j}{32\pi^3} \frac{(E/T_{\text{BH}})^2}{\exp(E/T_{\text{BH}}) \pm 1} S^{-\kappa} \Theta(t-t_q) \quad (3.1)$$

where the sign \pm corresponds to fermions and bosons, respectively. The factor $S^{-\kappa}$ ensures that the flux of the emitted particles is also modified by the memory burden, reflecting the change in the evaporation rate induced by the parameter κ . The number of particles emitted per unit time due to the evaporation can be calculated by integrating Eq. (3.1), over the energy, and it is given by

$$\frac{dN_{1j}}{dt} = \frac{27}{4} \frac{\xi g_j \zeta(3)}{16\pi^3} \frac{M_{\text{Pl}}^2}{M}, \quad (3.2)$$

$$\frac{dN_{2j}}{dt} = \frac{27}{4} \frac{\xi g_j \zeta(3) 2^k}{16\pi^3} \frac{M_{\text{Pl}}^{2+2\kappa}}{M^{1+2\kappa}} \quad (3.3)$$

where $\xi = 1$ for bosons and $\xi = 3/4$ for fermions. The quantities N_{1j} and N_{2j} denote the number of particles of species j produced during the semiclassical first phase and the subsequent quantum memory burden phase of evaporation, respectively.

To calculate the total number of particles produced through evaporation, one integrates the emission rate dN_j/dt over the lifetime of the PBH. In this context, two distinct scenarios arise: if the mass of the emitted particle satisfies $m_j < T_{\text{BH}}^0$, where T_{BH}^0 is the Hawking temperature of the PBH when the PBH start evaporating, then emission occurs throughout the entire lifetime of PBHs. On the other hand, if $m_j > T_{\text{BH}}^0$, production only begins at a later time t_j when the PBH temperature rises to satisfy $T_{\text{BH}}(t_j) = m_j$. One can find the time t_j to be

$$t_j = \begin{cases} t_{\text{ev}}^0 \left[1 - \frac{M_{\text{Pl}}^6}{M_{\text{in}}^3 m_j^3} \left(1 - \frac{\lambda_c \gamma}{2(1+w)} \right)^3 \right] & \text{for } t_j < t_q \\ t_{\text{ev}}^\kappa \left[1 - \left(\frac{M_{\text{Pl}}^2}{q M_{\text{in}} m_j} \right)^{3+2k} \left(1 - \frac{\lambda_c \gamma}{2(1+w)} \right)^{3+2\kappa} \right] & \text{for } t_j > t_q, \end{cases} \quad (3.4)$$

where t_q is the time after which memory burden starts dominating, defined before.

For the case of $m_j < T_{\text{BH}}^{\text{acc}}$, the DM will be produced throughout the time $[t_{\text{acc}}, t_{\text{ev}}^\kappa]$. One can calculate the number of particles produced in the semiclassical and memory burdened phase, N_{1j} and N_{2j} , by integrating Eq. (3.2) in the time interval $[t_{\text{acc}}, t_q]$ and Eq. (3.3) over the time interval $[t_q, t_{\text{ev}}^\kappa]$ respectively. For the detailed derivation regarding this, see our previous work [47]. In this paper, we also showed that for complete evaporation of PBHs, the total number of emitted particles is constant and does not depend on the rate of emission. The total number of DM particles with $m_j < T_{\text{BH}}^{\text{acc}}$, emitted from a single BH is thus given by

$$N_j = N_{1j} + N_{2j} = \frac{15\xi g_j \zeta(3)}{g_*(T_{\text{BH}}) \pi^4} \frac{M_{\text{in}}^2}{M_{\text{Pl}}^2} \left(1 - \frac{\lambda_c \gamma}{2(1+w)} \right)^{-2}, \quad (3.5)$$

which is the same as the total number of particles emitted from the Hawking evaporation, as expected. Similarly, for the case $m_j > T_{\text{BH}}^{\text{acc}}$, two scenarios can arise: $t_j < t_q$ and $t_j > t_q$. For $t_j < t_q$, N_{1j} and N_{2j} can be calculated by integrating Eqs. (3.2) and (3.3) over the time intervals $[t_j, t_q]$ and $[t_q, t_{\text{ev}}^\kappa]$ respectively. Whereas for $t_j > t_q$, $N_{1j} = 0$ and N_{2j} can be calculated by integrating over $[t_j, t_{\text{ev}}^\kappa]$. In both cases, after complete evaporation, we get the total number of DM particles emitted to be

$$N_j = N_{1j} + N_{2j} = \frac{15\xi g_j \zeta(3)}{g_*(T_{\text{BH}}) \pi^4} \frac{M_{\text{Pl}}^2}{m_j^2}. \quad (3.6)$$

The relic density of DM today is given by the ratio between the energy density of DM to the critical energy density of the universe as [95]

$$\Omega_j = \frac{\rho_j^0}{\rho_c^0} = \frac{S_0 n_j^{\text{re}}}{\rho_c^0 S_{\text{re}}} m_j \quad (3.7)$$

where $S_0 = 2.23 \times 10^{-38} \text{ GeV}^3$ is the entropy density of the universe today, and $\rho_c^0 = 5.15 \times 10^{-47} \text{ GeV}^4$ is the current critical energy density. The quantity n_j^{re} denotes the number density of the emitted DM particles at the end of reheating, and since the universe evolves adiabatically after reheating, the ratio n_j/S remains conserved. For a radiation-dominated universe, the entropy density is related to the temperature as $S_{\text{re}} = (25\pi^2/45)g_s^{\text{re}}T_{\text{re}}^3$, where g_s^{re} is the effective number of relativistic degrees of freedom contributing to entropy at the end of reheating. As mentioned before, we shall consider two scenarios: $\beta > \beta_{\text{cr}}$, when the energy density of PBHs dominates the energy density of the background, and $\beta < \beta_{\text{cr}}$ for which there will not be any PBH domination.

3.1 The case with $\beta > \beta_{\text{cr}}$

In this case, the energy density of the PBHs dominates the background. The reheating is governed solely by the evaporation of the PBHs. Hence, at the time of evaporation, the Hubble parameter behaves as $H_{\text{ev}} = 2/(3t_{\text{ev}}^\kappa)$. Further, as the reheating occurs due to the evaporation of PBHs, we get $\rho_{\text{R}}^{\text{re}} = \rho_{\text{BH}}^{\text{re}} = \rho_{\text{BH}}^{\text{ev}}$. The number density of DM is related to the number density of PBHs as $n_j^{\text{ev}} = N_j \times n_{\text{BH}}^{\text{ev}}$, where N_j is the number of particles emitted from the evaporation of a single PBH, and $n_{\text{BH}}^{\text{ev}}$ is the number density of PBHs at the time of evaporation. The quantity $n_{\text{BH}}^{\text{ev}}$ can be obtained as

$$n_{\text{BH}}^{\text{ev}} = \frac{4}{3} M_{\text{Pl}}^3 2^{2\kappa} (3 + 2\kappa)^2 \epsilon^2 \left(\frac{M_{\text{Pl}}}{qM_{\text{acc}}} \right)^{7+4\kappa}. \quad (3.8)$$

Finally using the expression of $n_{\text{BH}}^{\text{ev}}$ from Eq. (3.8) and the expressions of N_j from Eqs. (3.5) and (3.6), we obtain the relic abundance of DM for $m_j < T_{\text{BH}}^{\text{acc}}$ to be

$$\Omega_j h^2 = 2.43 \times 10^5 \frac{\xi g_j}{q^2} [2^\kappa (3 + 2\kappa)]^{1/2} \left(\frac{M_{\text{Pl}}}{qM_{\text{acc}}} \right)^{\frac{1+2\kappa}{2}} \frac{m_j}{\text{GeV}}, \quad (3.9)$$

and for $m_j > T_{\text{BH}}^{\text{acc}}$,

$$\Omega_j h^2 = 1.4 \times 10^{42} \xi g_j [2^\kappa (3 + 2\kappa)]^{1/2} \left(\frac{M_{\text{Pl}}}{qM_{\text{acc}}} \right)^{\frac{5+2\kappa}{2}} \frac{\text{GeV}}{m_j}. \quad (3.10)$$

In Fig. 3, we show the mass of DM produced from the evaporation of PBHs as a function of the initial mass of PBHs, for $w = 1/3$ (left panel) and $w = 2/3$ (right panel). The blue, green, and magenta lines correspond to memory burden parameters $\kappa = 0, 1, \text{ and } 2$, respectively. The shaded regions indicate an overproduction of DM, where $\Omega_j h^2 > 0.12$. The vertical lines mark the maximum initial masses of PBHs that can fully evaporate before the onset of BBN. We observe that as the memory burden parameter κ increases, the allowed parameter space in the $m_j - M_{\text{in}}$ plane becomes progressively smaller. Additionally, the solid, dashed, and dotted lines represent the cases of $\lambda_c = 0, \lambda_c^{\text{NR}}, \text{ and } \lambda_c^{\text{R}}$, respectively. From both panels, it is evident that the parameter space shrinks significantly in the case of relativistic accretion.

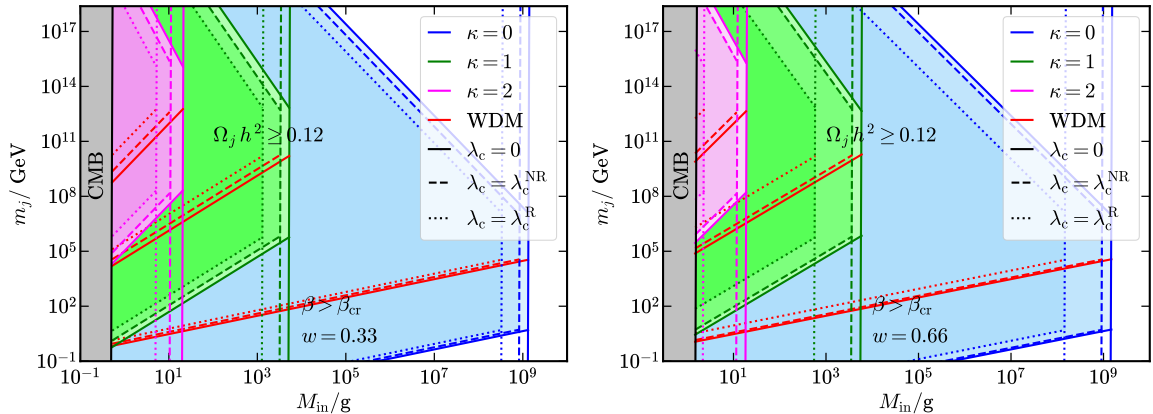


Figure 3. The mass of DM produced from the evaporation of PBHs is shown as a function of the initial mass of PBHs for the case $\beta > \beta_{\text{cr}}$. We consider two background equations of state: $w = 1/3$ displayed in the left panel, and $w = 2/3$ in the right panel. The grey shaded region corresponds to the minimum initial mass of PBHs set by the maximum energy scale of inflation, consistent with the current observational upper bound on the tensor-to-scalar ratio $r = 0.036$. The shaded colored regions indicate the parameter space that leads to an overproduction of DM, i.e. $\Omega_j, h^2 > 0.12$. The vertical lines mark the maximum initial mass of PBHs that ensures complete evaporation of PBHs before BBN. For both these plots, we fix $q = 1/2$. The blue, green, and magenta lines correspond to memory burden parameters $\kappa = 0, 1$, and 2 , respectively, while the solid, dashed, and dotted lines represent the cases $\lambda_c = 0, \lambda_c^{\text{NR}}$, and λ_c^{R} , respectively. The red lines represent the lower bounds on the DM mass, derived from warm DM constraints.

3.2 The case with $\beta < \beta_{\text{cr}}$

In this case, the energy density of PBHs never dominates over the background energy density of the universe. Several scenarios can arise in this context. For instance, PBHs may form and evaporate entirely during a phase dominated by the same background EoS. Alternatively, PBHs could form in a background with a general EoS and subsequently evaporate after the inflaton decays into radiation, leading to the epoch of radiation domination. As already stated, in this work we focus on the scenario where the coupling between the inflaton and radiation is small, resulting in an extended period of reheating. We also assume that reheating persists up to the onset of BBN. Additionally, we concentrate on PBHs that evaporate before BBN, thereby focusing on the first scenario described above. Let us begin with the case where the background is dominated by radiation. In this situation, the number density of PBHs at the time of evaporation is given by

$$n_{\text{BH}}^{\text{ev}} = 3\beta \left(\frac{\pi\gamma}{2}\right)^{1/2} [2^\kappa(3+2\kappa)\epsilon]^{3/2} M_{\text{Pl}}^3 \left(\frac{M_{\text{Pl}}}{M_{\text{in}}}\right)^{3/2} \left(\frac{M_{\text{Pl}}}{qM_{\text{acc}}}\right)^{\frac{3}{2}(3+2\kappa)}. \quad (3.11)$$

Further, during radiation domination using the relation between the energy density and temperature, $\rho_{\text{BH}}^{\text{ev}} = qM_{\text{acc}}n_{\text{BH}}^{\text{ev}} = \alpha T_{\text{ev}}^4$, we obtain that the temperature at the time of evaporation is given by

$$T_{\text{ev}} = \left(\frac{3}{4\alpha}\right)^{1/4} [2^\kappa(3+2\kappa)\epsilon]^{1/2} M_{\text{Pl}} \left(\frac{M_{\text{Pl}}}{qM_{\text{acc}}}\right)^{\frac{3+2\kappa}{2}}. \quad (3.12)$$

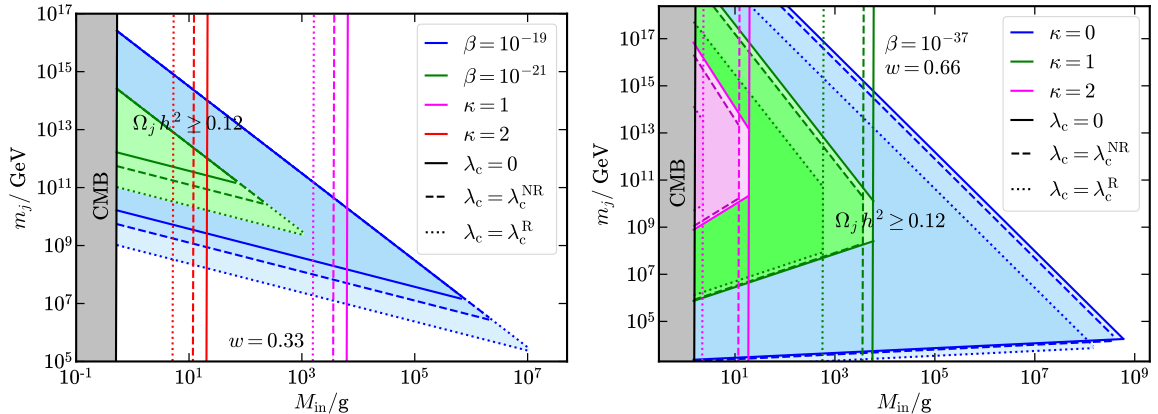


Figure 4. The mass of DM produced from the evaporation of PBHs is shown as a function of the initial mass of PBHs for the case $\beta < \beta_{\text{cr}}$. We consider two background equations of state: $w = 1/3$, displayed in the left panel, and $w = 2/3$, shown in the right panel. As before, the grey shaded region corresponds to the minimum initial mass of PBHs set by the maximum energy scale of inflation. The shaded colored regions indicate the parameter space that leads to an overproduction of DM, i.e. $\Omega_j, h^2 > 0.12$. In the left panel for $w = 1/3$, we present results for two values of β , where the blue and green lines correspond to $\beta = 10^{-19}$ and $\beta = 10^{-21}$, respectively. The vertical magenta and red lines denote the maximum initial masses allowed for complete evaporation of PBHs before BBN, for memory burden parameters $\kappa = 1$ and 2 , respectively. Throughout, we fix $q = 1/2$. In the right panel, for $w = 2/3$, we set $\beta = 10^{-37}$. Here, the blue, green, and magenta lines correspond to $\kappa = 0, 1$, and 2 , respectively. Finally, in both panels, the solid, dashed, and dotted lines represent the cases with $\lambda_c = 0, \lambda_c^{\text{NR}}$, and λ_c^{R} , respectively.

Using the relations given in Eqs. (3.11) and (3.12), we obtain the relic density of DM for $m_j < T_{\text{BH}}^{\text{acc}}$ to be

$$\Omega_j h^2 = 2.1 \times 10^5 \xi g_j \beta \left(\frac{M_{\text{in}}}{M_{\text{Pl}}} \right)^{1/2} \left(1 - \frac{3\lambda_c \gamma}{8} \right)^{-2} \frac{m_j}{\text{GeV}}. \quad (3.13)$$

Also for $m_j > T_{\text{BH}}^{\text{acc}}$ we have

$$\Omega_j h^2 = 1.28 \times 10^{42} \xi g_j \beta \left(\frac{M_{\text{Pl}}}{M_{\text{in}}} \right)^{3/2} \frac{\text{GeV}}{m_j}. \quad (3.14)$$

In Fig. 4, we illustrate on the left panel the parameter space of the mass of the emitted DM versus the initial mass of PBHs. We have chosen two different values of β , namely 10^{-19} (shown in blue) and 10^{-21} (shown in green). The shaded regions indicate where there is an overproduction of DM, i.e. $\Omega_j, h^2 > 0.12$. We observe that even a slight change in the parameter β significantly affects the allowed parameter space. From the relation for Ω_j, h^2 discussed earlier, it is clear that the memory burden parameter κ does not substantially modify the parameter space, except by restricting the maximum initial mass of PBHs that can evaporate before BBN. This is represented in the plot by the vertical magenta and red lines corresponding to $\kappa = 1$ and 2 , respectively. The solid, dashed, and dotted lines denote the cases with $\lambda_c = 0, \lambda_c^{\text{NR}}$, and λ_c^{R} , respectively. We also see that accretion significantly impacts the parameter space in the $m_j - M_{\text{in}}$ plane, reducing the allowed regions, particularly in the case of relativistic accretion.

Next, we consider the case where the background is governed by an EoS parameter w different from that of radiation. Given our assumption of a weak coupling between the inflaton and radiation, we focus on the scenario where reheating is driven by the evaporation of PBHs. In this context, PBHs may evaporate during the period of w -domination, thereby injecting radiation into the universe. For a stiffer background with $w > 1/3$, the energy density of the background fluid redshifts faster than the energy density of the radiation produced by the evaporation of PBHs. As a result, after a certain time, the energy density of radiation surpasses that of the background, effectively reheating the universe. Hence, for a background with w domination, the Hubble parameter at the time of evaporation is given by $H_{\text{ev}} = 2/[3(1+w)t_{\text{ev}}^\kappa]$. Further, the energy density of PBHs at the time of evaporation is given by

$$\rho_{\text{BH}}^{\text{ev}} = 48\pi^2 \beta M_{\text{Pl}}^4 \left[\frac{2^\kappa (3 + 2\kappa) \epsilon \gamma^w}{6\pi(1+w)} \right]^{\frac{2}{1+w}} \left(\frac{M_{\text{Pl}}}{M_{\text{in}}} \right)^{\frac{1+3w}{1+w}}. \quad (3.15)$$

At the point of evaporation, we have $\rho_{\text{BH}}^{\text{ev}} = \rho_{\text{R}}^{\text{ev}} = \alpha T_{\text{ev}}^4$. Using this, we obtain

$$\frac{n_{\text{BH}}^{\text{ev}}}{T_{\text{ev}}^3} = \frac{(\alpha^3 \rho_{\text{BH}}^{\text{ev}})^{1/4}}{q M_{\text{acc}}}. \quad (3.16)$$

Finally, we get an abundance of DM for $m_j < T_{\text{BH}}^{\text{acc}}$

$$\Omega_j h^2 = 4.8 \times 10^5 \frac{\xi g_j}{q^2} \left[\frac{2^\kappa (3 + 2\kappa) \epsilon \gamma^w}{6\pi(1+w)} \right]^{\frac{1}{2(1+w)}} \beta^{1/4} \left(\frac{M_{\text{Pl}}}{M_{\text{in}}} \right)^{\frac{1+3w}{4(1+w)}} \left(\frac{M_{\text{Pl}}}{q M_{\text{acc}}} \right)^{\frac{1-5w+4\kappa}{4(1+w)}} \frac{m_j}{\text{GeV}}, \quad (3.17)$$

and for $m_j > T_{\text{BH}}^{\text{acc}}$

$$\Omega_j h^2 = 2.9 \times 10^{42} \xi g_j \left[\frac{2^\kappa (3 + 2\kappa) \epsilon \gamma^w}{6\pi(1+w)} \right]^{\frac{1}{2(1+w)}} \beta^{1/4} \left(\frac{M_{\text{Pl}}}{M_{\text{in}}} \right)^{\frac{1+3w}{4(1+w)}} \left(\frac{M_{\text{Pl}}}{q M_{\text{acc}}} \right)^{\frac{9+3w+4\kappa}{4(1+w)}} \frac{\text{GeV}}{m_j}. \quad (3.18)$$

In Fig. 4, on the right panel, we illustrate the parameter space between the mass of emitted DM and the initial mass of PBHs, for the case where PBHs form and evaporate in a background with EoS $w = 2/3$. We assume a minimal reheating temperature of 40MeV, consistent with BBN constraints, and fix the initial PBH abundance to $\beta = 10^{-37}$. The shaded regions represent areas of DM overproduction. The blue, green, and magenta regions correspond to memory burden parameters $\kappa = 0, 1, \text{ and } 2$, respectively. As expected, increasing κ reduces the allowed parameter space due to the prolonged lifetime of PBHs. Additionally, the solid, dashed, and dotted lines correspond to $\lambda_c = 0, \lambda_c^{\text{NR}}, \text{ and } \lambda_c^{\text{R}}$, respectively. We see that accretion significantly impacts the viable parameter space of DM.

3.3 Constraints from warm dark matter

In this section, we aimed to satisfy the relic density of total DM of the universe from the particle j , emitted from the evaporation of PBHs. In such a case, one needs to simultaneously check that the particles are cold enough so that they do not destroy structure formation. The DM particles should have a minimum mass in order to stream freely, as constrained from Ly- α power spectra. On the other hand, such light DM is significantly constrained due to

the ultra-relativistic nature of the emitted particles. The lower bound on the mass of DM emitted from the evaporation of PBHs is given by [35, 92, 93]

$$m_j \geq 10^4 \langle E_{\text{eq}} \rangle, \quad (3.19)$$

where $\langle E_{\text{eq}} \rangle$ is the kinetic energy of the DM particles averaged over the temperature of PBHs. The average kinetic energy is further given by

$$\langle E_{\text{eq}} \rangle = \frac{a_{\text{ev}}}{a_{\text{eq}}} \langle E_{\text{ev}} \rangle = \delta T_{\text{BH}}^{\text{ev}} \left(\frac{g_{\text{s}}^{\text{eq}}}{g_{\text{s}}^{\text{ev}}} \right)^{1/3} \frac{T_{\text{eq}}}{T_{\text{ev}}} \quad (3.20)$$

where $g_{\text{s}}^{\text{eq}} = 3.94$ and $g_{\text{s}}^{\text{ev}} = 106.75$ are the relativistic degrees of freedom associated with entropy at the time of radiation-matter equality and at the time of evaporation. The quantity $T_{\text{eq}} = 0.75$ eV is the temperature at radiation-matter equality. The average kinetic energy at the time of evaporation is given in terms of the temperature of PBH at evaporation as $\langle E_{\text{ev}} \rangle = \delta T_{\text{BH}}^{\text{ev}}$, where $T_{\text{BH}}^{\text{ev}} = M_{\text{Pl}}^2 / (qM_{\text{acc}})$ and the parameter δ is taken to be $\delta \approx 1.3$. For the scenarios with PBH domination, the lower limit on the mass of emitted DM particles is given by

$$m_j \geq 0.02 \left(\frac{g_{\text{s}}^{\text{eq}}}{g_{\text{s}}^{\text{ev}}} \right)^{1/3} \frac{1}{\sqrt{2\kappa(3+2\kappa)\epsilon}} \left(\frac{qM_{\text{acc}}}{M_{\text{Pl}}} \right)^{\kappa+1/2}, \quad (3.21)$$

which is shown in the red lines in Fig. 3.

4 Dard matter from stable PBHs

As is now well understood, memory burden effects can stabilise lower-mass PBHs, allowing them to survive until the present universe. In most cases, the initial part of the Hawking evaporation of the PBHs has already occurred before BBN. Therefore, in principle, the total relic abundance of DM should include contributions from both the evaporated component and the remnant sector. However, the contribution from evaporation is typically subdominant compared to that of the remnant, unless the value of the parameter q is very small (e.g., $q \lesssim 10^{-2}$); see [47] for details. Since we primarily focus on the case $q = 1/2$, the contribution from evaporation can be safely neglected. The dimensionless energy density parameter for the surviving PBHs is then given by

$$\Omega_{\text{PBH}} = \frac{\rho_{\text{BH}}^0}{\rho_{\text{c}}^0} = 5.62 \times 10^9 \frac{g_0}{g_{\text{re}}} \frac{qM_{\text{acc}} n_{\text{BH}}^{\text{re}}}{\alpha T_{\text{re}}^3}, \quad (4.1)$$

where g_0 and g_{re} are the relativistic degrees of freedom at present day and at the time of reheating. The number density of PBHs at the time of reheating is given by

$$n_{\text{BH}}^{\text{re}} = \beta \frac{\rho_w^{\text{in}}}{M_{\text{in}}} \left(\frac{a_{\text{in}}}{a_{\text{re}}} \right)^3, \quad (4.2)$$

with ρ_w^{in} being the energy density of the background at the time of the formation of PBHs. Next, the ratio of the scale factor during a w -dominated phase can be obtained as

$$\left(\frac{a_{\text{in}}}{a_{\text{re}}} \right)^3 = \left(\frac{t_{\text{in}}}{t_{\text{re}}} \right)^{\frac{2}{1+w}} = \left(\frac{\alpha}{48\pi^2} \right)^{\frac{1}{1+w}} \gamma^{-\frac{2}{1+w}} \left(\frac{T_{\text{re}}}{M_{\text{Pl}}} \right)^{\frac{4}{1+w}} \left(\frac{M_{\text{in}}}{M_{\text{Pl}}} \right)^{\frac{2}{1+w}}. \quad (4.3)$$

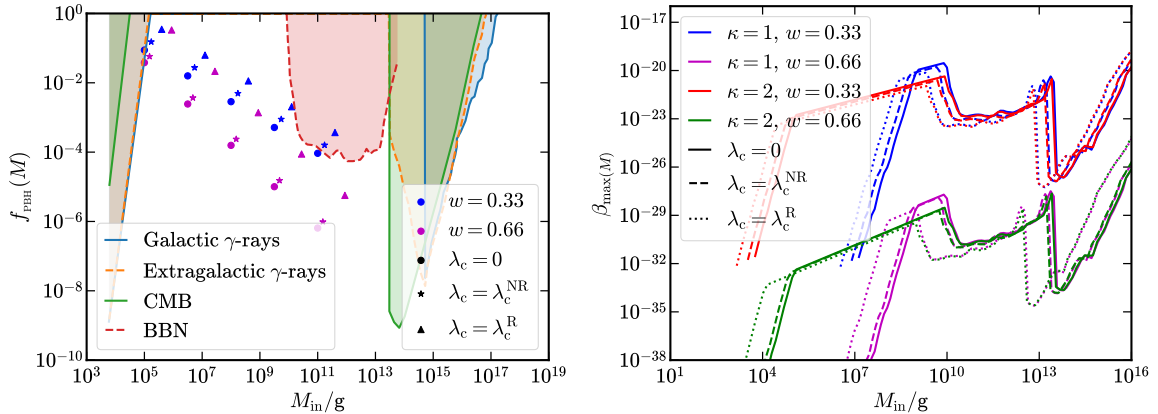


Figure 5. The fraction of today’s DM energy density sourced by PBHs, denoted by f_{PBH} , is shown as a function of the PBH mass in the left panel. The contours represent observational constraints on the maximum allowed value of f_{PBH} from various experiments. The blue and magenta points correspond to cases where the EoS at the time of PBH formation is $w = 1/3$, $\beta = 10^{-23}$ and $w = 2/3$, $\beta = 10^{-33}$, respectively. The circular points indicate scenarios with no accretion ($\lambda_c = 0$), while the corresponding starred and triangular points represent the cases with λ_c^{NR} and λ_c^{R} , respectively. Since accretion alters the PBH mass and thereby modifies f_{PBH} , the observational constraints on f_{PBH} translate into different bounds on the initial PBH abundance β . These constraints on β are shown in the right panel. Here, the cases with $\kappa = 1$ are illustrated by blue and magenta curves, while $\kappa = 2$ is shown by red and green curves. Moreover, the results for $w = 1/3$ are plotted in blue and red, whereas those for $w = 2/3$ are given by magenta and green curves.

Finally, the dimensionless density parameter has the following form

$$\Omega_{\text{PBH}} = 5.16 \times 10^{26} \beta \frac{q M_{\text{acc}}}{M_{\text{in}}} \left(\frac{48\pi^2}{\alpha} \right)^{\frac{w}{1+w}} \gamma^{\frac{2w}{1+\epsilon}} \left(\frac{T_{\text{re}}}{M_{\text{Pl}}} \right)^{\frac{1-3w}{1+w}} \left(\frac{M_{\text{in}}}{M_{\text{Pl}}} \right)^{-\frac{2w}{1+w}}. \quad (4.4)$$

An important point is that for $w = 1/3$, Ω_{PBH} becomes independent of the temperature of reheating. And if the PBHs form during an epoch of w -domination, Ω_{PBH} behaves with the PBH mass as $\Omega_{\text{PBH}} \propto M_{\text{in}}^{-2w/(1+w)}$. Another important quantity related to stable PBHs is f_{PBH} , which is defined as what fraction of the DM energy density today that comes from PBHs, and it is given by $f_{\text{PBH}} = \Omega_{\text{PBH}}/0.12$. In Fig. 5, on the left panel, we have illustrated the values of f_{PBH} as a function of the mass of PBHs. We have chosen different initial masses and plotted the corresponding f_{PBH} for three cases: $\lambda_c = 0$, λ_c^{NR} , and λ_c^{R} , which are shown using circular, starred, and triangular markers, respectively. The colours blue and magenta represent two background equations of state, $w = 1/3$ and $w = 2/3$, respectively. The mass-dependent observational constraints are shown by the contours above. We observe that for $\lambda_c = \lambda_c^{\text{R}}$, the shift in both the mass and f_{PBH} is quite significant. This implies that for a PBH with a given initial mass, even if the corresponding f_{PBH} is within allowed limits in the absence of accretion, the scenario may be ruled out due to accretion-induced mass growth. It is important to note that the accretion phase occurs much earlier than the evaporation timescale. Therefore, the observational constraints on f_{PBH} depend only on the final mass of PBHs and are unaffected directly by the process of accretion. However, since accretion modifies the mapping between initial mass and final mass, and hence alters f_{PBH} , it leads to different constraints on the initial abundance of PBHs β , which are shown in the right panel of Fig. 5. We find that due

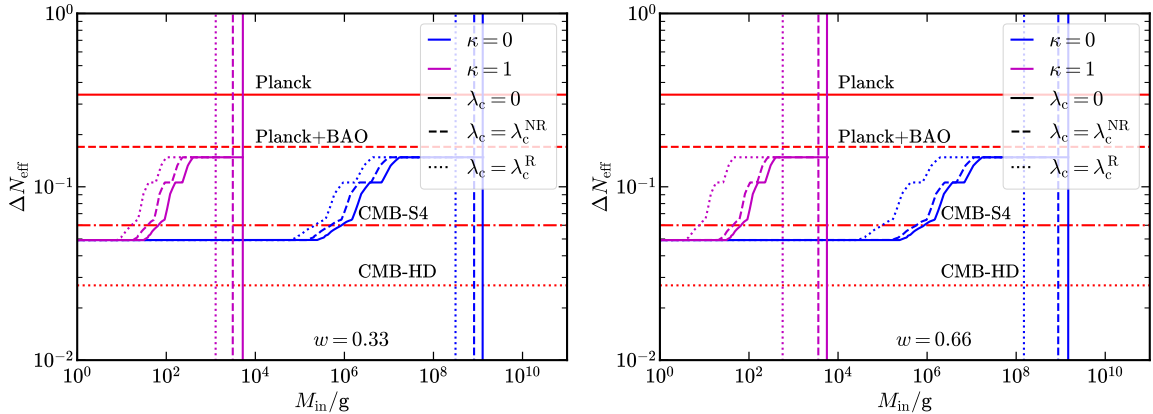


Figure 6. The contribution to ΔN_{eff} from spin-0 bosonic particles generated from the evaporation of PBHs is shown as a function of the initial mass of PBHs, for two different backgrounds where the PBHs have formed, i.e. $w = 1/3$ (left panel) and $w = 2/3$ (right panel), respectively. The red solid, dashed, dot-dashed, and dotted lines correspond to the bounds on ΔN_{eff} given by observations from Planck, Planck+BAO, CMB-S4, and CMB-HD. The blue and magenta lines correspond to two different choices of the memory burden parameters, $\kappa = 0$, $q = 1$ and $\kappa = 1$, $q = 1/2$, respectively. The vertical lines represent the maximum limit on the formation mass that ensures complete evaporation of PBHs before BBN. As usual, the cases of $\lambda_c = 0$, λ_c^{NR} , and λ_c^{R} are shown with solid, dashed, and dotted lines, respectively.

to accretion, the maximum allowed value of β for a given M_{in} can vary by several orders of magnitude.

5 Dark radiation from the evaporation of PBHs

As the PBHs evaporate, along with SM particles, other species such as DM, right-handed neutrinos, and DR can also be produced. DR refers to light, feebly interacting particles that remain relativistic during early cosmic epochs and thus contribute to the total radiation energy density at the time of BBN or even during recombination. The presence of such DR is commonly characterised by its contribution to the effective number of relativistic degrees of freedom, denoted by the quantity ΔN_{eff} , which is defined as [93]

$$\Delta N_{\text{eff}} = \frac{\rho_{\text{DR}}^{\text{eq}}}{\rho_{\text{R}}^{\text{eq}}} \left[N_{\nu} + \frac{8}{7} \left(\frac{11}{4} \right)^{4/3} \right], \quad (5.1)$$

where $\rho_{\text{DR}}^{\text{eq}}$ and $\rho_{\text{R}}^{\text{eq}}$ are the energy density of DR and radiation at the time of radiation-matter equality, and $N_{\nu} = 3.045$ is the effective number of neutrino species [96–104]. Using the conservation of entropy, as defined before, the ratio of the energy densities given by

$$\frac{\rho_{\text{DR}}^{\text{eq}}}{\rho_{\text{R}}^{\text{eq}}} = \frac{g_{\text{ev}}}{g_{\text{eq}}} \left(\frac{g_{\text{s}}^{\text{eq}}}{g_{\text{s}}^{\text{ev}}} \right)^{4/3} \frac{\rho_{\text{DR}}^{\text{ev}}}{\rho_{\text{R}}^{\text{ev}}}, \quad (5.2)$$

where g_{ev} and g_{eq} are the relativistic degrees of freedom and g_{s}^{ev} and g_{s}^{eq} are relativistic degrees of freedom associated with entropy at the time of evaporation and at radiation-matter equality, respectively. For the scenario with PBH domination, we get $\rho_{\text{DR}}^{\text{eq}}/\rho_{\text{R}}^{\text{eq}} = g_{\text{DR}}^{\text{H}}/g_{\text{H}}$, and

hence Eq. (5.1) reads [93]

$$\Delta N_{\text{eff}} = \frac{g_{\text{ev}}}{g_{\text{eq}}} \left(\frac{g_{\text{s}}^{\text{eq}}}{g_{\text{s}}^{\text{ev}}} \right)^{4/3} \frac{g_{\text{DR}}^{\text{H}}}{g_{\text{H}}} \left[N_{\nu} + \frac{8}{7} \left(\frac{11}{4} \right)^{4/3} \right], \quad (5.3)$$

where $g_{\text{DR}}^{\text{H}} = 4, 2, 1.82, 1.23, 0.05$ for Dirac and Weyl fermion, scalar and vector boson, and massless graviton, respectively. Observation of CMB currently restricts ΔN_{eff} to $\Delta N_{\text{eff}} = 0.34$ [105], whereas combined with data of baryon acoustic oscillation (BAO), the constraint improves to $N_{\text{eff}} = 2.99 \pm 0.17$. Further, forthcoming CMB missions such as CMB-S4 [106], CMB-HD [107] are expected to measure ΔN_{eff} with more precisions of $\Delta N_{\text{eff}} = 0.06$, and $\Delta N_{\text{eff}} = 0.027$, respectively. In Fig. 6, we have shown the contribution to ΔN_{eff} from the spin-0 bosonic components for the case of PBH domination. In the case of ΔN_{eff} , the detailed behaviour of g_{s}^{ev} with T_{ev} is required, where for the case of PBH domination, the temperature at evaporation reads $T_{\text{ev}} = [(4/(3\alpha))M_{\text{Pl}}^4 2^{2\kappa} (3 + 2\kappa)^2 \epsilon^2 (M_{\text{Pl}}/(qM_{\text{acc}}))^{6+4\kappa}]^{1/4}$. The blue and magenta lines correspond to $\kappa = 0, q = 1$ and $\kappa = 1, q = 1/2$, respectively, while the solid, dashed, and dotted lines correspond to $\lambda_{\text{c}} = 0, \lambda_{\text{c}}^{\text{NR}}$, and $\lambda_{\text{c}}^{\text{R}}$. In the figure, we have illustrated the case for a single component with $g_{\text{DR}}^{\text{H}} = 1.82$, as our aim is to show the effects of κ and w . Contributions from other sectors with different values of g_{DR}^{H} will have similar qualitative effects. It can be shown that the upcoming observations from CMB-S4 or CMB-HD might be able to rule out all components except the massless graviton as contributors to DR.

6 Conclusions

In this work, we have examined the effects of relativistic accretion and burdened evaporation on the evolution of PBHs. The quantum memory burden effect, which induces a backreaction on the process of evaporation, causes PBHs to persist for a longer duration. On the other hand, accretion of relativistic particles can lead to a substantial growth in the initial mass of PBHs, allowing them to survive even longer (see Figs. 1 and 2). Our primary aim was to investigate the joint effects of these two processes in the context of various phenomena, which we summarise below.

We considered PBHs with an initial mass range such that they are expected to have evaporated before BBN. Throughout this work, we have explored two choices for the background EoS, namely $w = 1/3$ and a stiffer EoS $w = 2/3$, as toy examples. We focused on scenarios where the evaporation of PBHs leads to the production of DM particles. For the evaporation process, we analysed two distinct cases characterised by the critical value of the initial abundance of PBHs, β . When $\beta > \beta_{\text{cr}}$, the energy density of PBHs dominates over the background energy density before evaporation, whereas for $\beta < \beta_{\text{cr}}$, the energy density of PBHs remains subdominant. For the case $\beta < \beta_{\text{cr}}$, we further considered a scenario where the background is governed by $w > 1/3$, and reheating is achieved when the radiation generated from the evaporation of PBHs eventually dominates the background energy density. We demonstrated that increasing the memory burden parameter κ significantly reduces the available parameter space in the $m_j - M_{\text{in}}$ plane for the emitted mass of DM and the initial mass of PBHs (see Figs. 3 and 4). Including the effects of accretion further shrinks this parameter space, with relativistic accretion leading to particularly pronounced reductions. Additionally, we provided constraints on the $m_j - M_{\text{in}}$ parameter space arising from warm DM.

We further considered the mass ranges of PBHs and the memory burden parameters for which PBHs can survive until the present epoch. We calculated the fraction of the total DM

given by PBHs, denoted by f_{PBH} , and examined the impacts of both accretion and burdened evaporation on f_{PBH} . We demonstrated that while the memory burden effect opens up a new window of f_{PBH} for smaller masses of PBHs, accretion shifts both the mass of PBHs and the corresponding value of f_{PBH} s to higher values for a given initial mass. Building on this, we explored how accretion influences the required initial abundance of PBHs, and provided the resulting constraints from various mass-dependent observational limits on f_{PBH} (see Fig. 5).

Lastly, we considered the emission of DR from the evaporation of PBHs and examined their effects on ΔN_{eff} , (see Fig. 6), especially when the effects of accretion and memory burden are considered.

Acknowledgments

SM thanks the Indian Institute of Science Education and Research (IISER), Pune, for support through a postdoctoral fellowship.

References

- [1] B. J. Carr and S. W. Hawking, *Black holes in the early Universe*, *Mon. Not. Roy. Astron. Soc.* **168** (1974) 399–415.
- [2] S. Hawking, *Gravitationally collapsed objects of very low mass*, *Mon. Not. Roy. Astron. Soc.* **152** (1971) 75.
- [3] P. Ivanov, P. Naselsky, and I. Novikov, *Inflation and primordial black holes as dark matter*, *Phys. Rev. D* **50** (1994) 7173–7178.
- [4] N. Bartolo, V. De Luca, G. Franciolini, A. Lewis, M. Peloso, and A. Riotto, *Primordial Black Hole Dark Matter: LISA Serendipity*, *Phys. Rev. Lett.* **122** (2019), no. 21 211301, [[arXiv:1810.12218](#)].
- [5] B. Carr and F. Kuhnel, *Primordial Black Holes as Dark Matter: Recent Developments*, *Ann. Rev. Nucl. Part. Sci.* **70** (2020) 355–394, [[arXiv:2006.02838](#)].
- [6] K. Jedamzik, *Primordial Black Hole Dark Matter and the LIGO/Virgo observations*, *JCAP* **09** (2020) 022, [[arXiv:2006.11172](#)].
- [7] K. Jedamzik, *Consistency of Primordial Black Hole Dark Matter with LIGO/Virgo Merger Rates*, *Phys. Rev. Lett.* **126** (2021), no. 5 051302, [[arXiv:2007.03565](#)].
- [8] A. M. Green and B. J. Kavanagh, *Primordial Black Holes as a dark matter candidate*, *J. Phys. G* **48** (2021), no. 4 043001, [[arXiv:2007.10722](#)].
- [9] P. Villanueva-Domingo, O. Mena, and S. Palomares-Ruiz, *A brief review on primordial black holes as dark matter*, *Front. Astron. Space Sci.* **8** (2021) 87, [[arXiv:2103.12087](#)].
- [10] B. Carr and F. Kuhnel, *Primordial black holes as dark matter candidates*, *SciPost Phys. Lect. Notes* **48** (2022) 1, [[arXiv:2110.02821](#)].
- [11] R.-g. Cai, S. Pi, and M. Sasaki, *Gravitational Waves Induced by non-Gaussian Scalar Perturbations*, *Phys. Rev. Lett.* **122** (2019), no. 20 201101, [[arXiv:1810.11000](#)].
- [12] **LIGO Scientific, Virgo** Collaboration, B. P. Abbott et al., *Observation of Gravitational Waves from a Binary Black Hole Merger*, *Phys. Rev. Lett.* **116** (2016), no. 6 061102, [[arXiv:1602.03837](#)].
- [13] **LIGO Scientific, Virgo** Collaboration, B. P. Abbott et al., *Binary Black Hole Mergers in the first Advanced LIGO Observing Run*, *Phys. Rev. X* **6** (2016), no. 4 041015, [[arXiv:1606.04856](#)]. [Erratum: *Phys.Rev.X* 8, 039903 (2018)].

- [14] **LIGO Scientific, Virgo** Collaboration, B. P. Abbott et al., *The basic physics of the binary black hole merger GW150914*, *Annalen Phys.* **529** (2017), no. 1-2 1600209, [[arXiv:1608.01940](#)].
- [15] **LIGO Scientific, VIRGO** Collaboration, B. P. Abbott et al., *GW170104: Observation of a 50-Solar-Mass Binary Black Hole Coalescence at Redshift 0.2*, *Phys. Rev. Lett.* **118** (2017), no. 22 221101, [[arXiv:1706.01812](#)]. [Erratum: *Phys.Rev.Lett.* 121, 129901 (2018)].
- [16] **LIGO Scientific, Virgo** Collaboration, B. P. Abbott et al., *GW170814: A Three-Detector Observation of Gravitational Waves from a Binary Black Hole Coalescence*, *Phys. Rev. Lett.* **119** (2017), no. 14 141101, [[arXiv:1709.09660](#)].
- [17] **LIGO Scientific, Virgo** Collaboration, B. . P. . Abbott et al., *GW170608: Observation of a 19-solar-mass Binary Black Hole Coalescence*, *Astrophys. J. Lett.* **851** (2017) L35, [[arXiv:1711.05578](#)].
- [18] **NANOGrav** Collaboration, G. Agazie et al., *The NANOGrav 15 yr Data Set: Evidence for a Gravitational-wave Background*, *Astrophys. J. Lett.* **951** (2023), no. 1 L8, [[arXiv:2306.16213](#)].
- [19] **NANOGrav** Collaboration, G. Agazie et al., *The NANOGrav 15 yr Data Set: Observations and Timing of 68 Millisecond Pulsars*, *Astrophys. J. Lett.* **951** (2023), no. 1 L9, [[arXiv:2306.16217](#)].
- [20] **EPTA** Collaboration, J. Antoniadis et al., *The second data release from the European Pulsar Timing Array - I. The dataset and timing analysis*, *Astron. Astrophys.* **678** (2023) A48, [[arXiv:2306.16224](#)].
- [21] **EPTA, InPTA:** Collaboration, J. Antoniadis et al., *The second data release from the European Pulsar Timing Array - III. Search for gravitational wave signals*, *Astron. Astrophys.* **678** (2023) A50, [[arXiv:2306.16214](#)].
- [22] A. Zic et al., *The Parkes Pulsar Timing Array third data release*, *Publ. Astron. Soc. Austral.* **40** (2023) e049, [[arXiv:2306.16230](#)].
- [23] D. J. Reardon et al., *Search for an Isotropic Gravitational-wave Background with the Parkes Pulsar Timing Array*, *Astrophys. J. Lett.* **951** (2023), no. 1 L6, [[arXiv:2306.16215](#)].
- [24] H. Xu et al., *Searching for the Nano-Hertz Stochastic Gravitational Wave Background with the Chinese Pulsar Timing Array Data Release I*, *Res. Astron. Astrophys.* **23** (2023), no. 7 075024, [[arXiv:2306.16216](#)].
- [25] S. W. Hawking, *Black hole explosions*, *Nature* **248** (1974) 30–31.
- [26] S. W. Hawking, *Particle Creation by Black Holes*, *Commun. Math. Phys.* **43** (1975) 199–220. [Erratum: *Commun.Math.Phys.* 46, 206 (1976)].
- [27] M. Riajul Haque, E. Kpatcha, D. Maity, and Y. Mambrini, *Primordial black hole reheating*, *Phys. Rev. D* **108** (2023), no. 6 063523, [[arXiv:2305.10518](#)].
- [28] S. Maity and M. R. Haque, *Probing the early universe with future GW observatories*, *JCAP* **04** (2025) 091, [[arXiv:2407.18246](#)].
- [29] A. M. Green, *Supersymmetry and primordial black hole abundance constraints*, *Phys. Rev. D* **60** (1999) 063516, [[astro-ph/9903484](#)].
- [30] A. Cheek, L. Heurtier, Y. F. Perez-Gonzalez, and J. Turner, *Primordial black hole evaporation and dark matter production. I. Solely Hawking radiation*, *Phys. Rev. D* **105** (2022), no. 1 015022, [[arXiv:2107.00013](#)].
- [31] A. Cheek, L. Heurtier, Y. F. Perez-Gonzalez, and J. Turner, *Primordial black hole evaporation and dark matter production. II. Interplay with the freeze-in or freeze-out mechanism*, *Phys. Rev. D* **105** (2022), no. 1 015023, [[arXiv:2107.00016](#)].
- [32] N. Bernal, Y. F. Perez-Gonzalez, and Y. Xu, *Superradiant production of heavy dark matter from primordial black holes*, *Phys. Rev. D* **106** (2022), no. 1 015020, [[arXiv:2205.11522](#)].

- [33] D. Hooper, G. Krnjaic, and S. D. McDermott, *Dark Radiation and Superheavy Dark Matter from Black Hole Domination*, *JHEP* **08** (2019) 001, [[arXiv:1905.01301](#)].
- [34] I. Masina, *Dark matter and dark radiation from evaporating primordial black holes*, *Eur. Phys. J. Plus* **135** (2020), no. 7 552, [[arXiv:2004.04740](#)].
- [35] B. Barman, M. R. Haque, and Ó. Zapata, *Gravitational wave signatures of cogenesis from a burdened PBH*, *JCAP* **09** (2024) 020, [[arXiv:2405.15858](#)].
- [36] R. Dong, W. H. Kinney, and D. Stojkovic, *Gravitational wave production by Hawking radiation from rotating primordial black holes*, *JCAP* **10** (2016) 034, [[arXiv:1511.05642](#)].
- [37] S. Sugiyama, V. Takhistov, E. Vitagliano, A. Kusenko, M. Sasaki, and M. Takada, *Testing Stochastic Gravitational Wave Signals from Primordial Black Holes with Optical Telescopes*, *Phys. Lett. B* **814** (2021) 136097, [[arXiv:2010.02189](#)].
- [38] K. Inomata, M. Kawasaki, K. Mukaida, T. Terada, and T. T. Yanagida, *Gravitational Wave Production right after a Primordial Black Hole Evaporation*, *Phys. Rev. D* **101** (2020), no. 12 123533, [[arXiv:2003.10455](#)].
- [39] G. Domènech, V. Takhistov, and M. Sasaki, *Exploring evaporating primordial black holes with gravitational waves*, *Phys. Lett. B* **823** (2021) 136722, [[arXiv:2105.06816](#)].
- [40] A. Ireland, S. Profumo, and J. Scharnhorst, *Primordial gravitational waves from black hole evaporation in standard and nonstandard cosmologies*, *Phys. Rev. D* **107** (2023), no. 10 104021, [[arXiv:2302.10188](#)].
- [41] G. Dvali and C. Gomez, *Black Holes as Critical Point of Quantum Phase Transition*, *Eur. Phys. J. C* **74** (2014) 2752, [[arXiv:1207.4059](#)].
- [42] M. Michel and S. Zell, *The Timescales of Quantum Breaking*, *Fortsch. Phys.* **71** (2023) 2300163, [[arXiv:2306.09410](#)].
- [43] S.-J. Wang, *The doomsday of black hole evaporation*, *EPL* **146** (2024), no. 3 39002, [[arXiv:2308.07909](#)].
- [44] G. Dvali, L. Eisemann, M. Michel, and S. Zell, *Black hole metamorphosis and stabilization by memory burden*, *Phys. Rev. D* **102** (2020), no. 10 103523, [[arXiv:2006.00011](#)].
- [45] A. Alexandre, G. Dvali, and E. Koutsangelas, *New mass window for primordial black holes as dark matter from the memory burden effect*, *Phys. Rev. D* **110** (2024), no. 3 036004, [[arXiv:2402.14069](#)].
- [46] V. Thoss, A. Burkert, and K. Kohri, *Breakdown of hawking evaporation opens new mass window for primordial black holes as dark matter candidate*, *Mon. Not. Roy. Astron. Soc.* **532** (2024), no. 1 451–459, [[arXiv:2402.17823](#)].
- [47] M. R. Haque, S. Maity, D. Maity, and Y. Mambrini, *Quantum effects on the evaporation of PBHs: contributions to dark matter*, *JCAP* **07** (2024) 002, [[arXiv:2404.16815](#)].
- [48] A. Chaudhuri, K. Kohri, and V. Thoss, *New bounds on Memory Burdened Primordial Black Holes from Big Bang Nucleosynthesis*, [[arXiv:2506.20717](#)].
- [49] A. Moursy and Q. Shafi, *Primordial monopoles, black holes and gravitational waves*, *JCAP* **08** (2024) 064, [[arXiv:2405.04397](#)].
- [50] N. Bhaumik, M. R. Haque, R. K. Jain, and M. Lewicki, *Memory burden effect mimics reheating signatures on SGWB from ultra-low mass PBH domination*, *JHEP* **10** (2024) 142, [[arXiv:2409.04436](#)].
- [51] K. Kohri, T. Terada, and T. T. Yanagida, *Induced gravitational waves probing primordial black hole dark matter with the memory burden effect*, *Phys. Rev. D* **111** (2025), no. 6 063543, [[arXiv:2409.06365](#)].

- [52] Y. Jiang, C. Yuan, C.-Z. Li, and Q.-G. Huang, *Constraints on the primordial black hole abundance through scalar-induced gravitational waves from Advanced LIGO and Virgo's first three observing runs*, *JCAP* **12** (2024) 016, [[arXiv:2409.07976](#)].
- [53] W. Barker, B. Gladwyn, and S. Zell, *Inflationary and gravitational wave signatures of small primordial black holes as dark matter*, *Phys. Rev. D* **111** (2025), no. 12 123033, [[arXiv:2410.11948](#)].
- [54] M. Gross, Y. Mambrini, E. Kpatcha, M. O. Olea-Romacho, and R. Roshan, *Gravitational wave production during reheating: From the inflaton to primordial black holes*, *Phys. Rev. D* **111** (2025), no. 3 035020, [[arXiv:2411.04189](#)].
- [55] P. Athron, M. Chianese, S. Datta, R. Samanta, and N. Saviano, *Impact of memory-burdened black holes on primordial gravitational waves in light of Pulsar Timing Array*, *JCAP* **05** (2025) 005, [[arXiv:2411.19286](#)].
- [56] A. K. Saha, A. Singh, P. Parashari, and R. Laha, *Hunting Primordial Black Hole Dark Matter in Lyman- α Forest*, [arXiv:2409.10617](#).
- [57] N. P. D. Loc, *Gravitational waves from burdened primordial black holes dark matter*, *Phys. Rev. D* **111** (2025), no. 2 023509, [[arXiv:2410.17544](#)].
- [58] D. Borah and N. Das, *Successful co genesis of baryon and dark matter from memory-burdened PBH*, *JCAP* **02** (2025) 031, [[arXiv:2410.16403](#)].
- [59] G. Montefalcone, D. Hooper, K. Freese, C. Kelso, F. Kuhnel, and P. Sandick, *Does Memory Burden Open a New Mass Window for Primordial Black Holes as Dark Matter?*, [arXiv:2503.21005](#).
- [60] G. Dvali, M. Zantedeschi, and S. Zell, *Transitioning to Memory Burden: Detectable Small Primordial Black Holes as Dark Matter*, [arXiv:2503.21740](#).
- [61] A. Takeshita and T. Kitabayashi, *WIMP/FIMP dark matter and primordial black holes with memory burden effect*, [arXiv:2506.20071](#).
- [62] V. De Romeri, Y. F. Perez-Gonzalez, and A. Tolino, *Primordial black hole probes of heavy neutral leptons*, *JCAP* **04** (2025) 018, [[arXiv:2405.00124](#)].
- [63] M. Chianese, A. Boccia, F. Iocco, G. Miele, and N. Saviano, *Light burden of memory: Constraining primordial black holes with high-energy neutrinos*, *Phys. Rev. D* **111** (2025), no. 6 063036, [[arXiv:2410.07604](#)].
- [64] R. Calabrese, M. Chianese, and N. Saviano, *Impact of memory-burdened primordial black holes on high-scale leptogenesis*, *Phys. Rev. D* **111** (2025), no. 8 083008, [[arXiv:2501.06298](#)].
- [65] G. Dvali, J. S. Valbuena-Bermúdez, and M. Zantedeschi, *Memory burden effect in black holes and solitons: Implications for PBH*, *Phys. Rev. D* **110** (2024), no. 5 056029, [[arXiv:2405.13117](#)].
- [66] C. J. Shallue, J. B. Muñoz, and G. Z. Krnjaic, *Warm Hawking relics from primordial black hole domination*, *JCAP* **02** (2025) 026, [[arXiv:2406.08535](#)].
- [67] M. Zantedeschi and L. Visinelli, *Ultralight Black Holes as Sources of High-Energy Particles*, [arXiv:2410.07037](#).
- [68] U. Basumatary, N. Raj, and A. Ray, *Beyond Hawking evaporation of black holes formed by dark matter in compact stars*, *Phys. Rev. D* **111** (2025), no. 4 L041306, [[arXiv:2410.22702](#)].
- [69] B. Barman, K. Loho, and Ó. Zapata, *Asymmetries from a charged memory-burdened PBH*, *JCAP* **02** (2025) 052, [[arXiv:2412.13254](#)].
- [70] D. Bandyopadhyay, D. Borah, and N. Das, *Axion misalignment with memory-burdened PBH*, *JCAP* **04** (2025) 039, [[arXiv:2501.04076](#)].

- [71] A. Boccia and F. Iocco, *A strike of luck: could the KM3-230213A event be caused by an evaporating primordial black hole?*, [arXiv:2502.19245](#).
- [72] M. Chianese, *High-energy gamma-ray emission from memory-burdened primordial black holes*, [arXiv:2504.03838](#).
- [73] X.-h. Tan and Y.-f. Zhou, *Probing Memory-Burdened Primordial Black Holes with Galactic Sources observed by LHAASO*, [arXiv:2505.19857](#).
- [74] A. Dondarini, G. Marino, P. Panci, and M. Zantedeschi, *The fast, the slow and the merging: probes of evaporating memory burdened PBHs*, [arXiv:2506.13861](#).
- [75] H. Bondi, *On spherically symmetrical accretion*, *Mon. Not. Roy. Astron. Soc.* **112** (1952) 195.
- [76] T. Harada and B. J. Carr, *Growth of primordial black holes in a universe containing a massless scalar field*, *Phys. Rev. D* **71** (2005) 104010, [[astro-ph/0412135](#)].
- [77] T. Harada and B. J. Carr, *Upper limits on the size of a primordial black hole*, *Phys. Rev. D* **71** (2005) 104009, [[astro-ph/0412134](#)].
- [78] F. D. Lora-Clavijo, F. S. Guzmán, and A. Cruz-Osorio, *PBH mass growth through radial accretion during the radiation dominated era*, *JCAP* **12** (2013) 015, [[arXiv:1312.0989](#)].
- [79] K. J. Mack, J. P. Ostriker, and M. Ricotti, *Growth of structure seeded by primordial black holes*, *Astrophys. J.* **665** (2007) 1277–1287, [[astro-ph/0608642](#)].
- [80] I. K. Dhihingia, S. Das, D. Maity, and S. Chakrabarti, *Limitations of the pseudo-Newtonian approach in studying the accretion flow around a Kerr black hole*, *Phys. Rev. D* **98** (2018), no. 8 083004, [[arXiv:1806.08481](#)].
- [81] V. De Luca, G. Franciolini, P. Pani, and A. Riotto, *Constraints on Primordial Black Holes: the Importance of Accretion*, *Phys. Rev. D* **102** (2020), no. 4 043505, [[arXiv:2003.12589](#)].
- [82] V. De Luca, G. Franciolini, A. Kehagias, P. Pani, and A. Riotto, *Primordial black holes in matter-dominated eras: The role of accretion*, *Phys. Lett. B* **832** (2022) 137265, [[arXiv:2112.02534](#)].
- [83] Y. Yang, *Influences of accreting primordial black holes on the global 21 cm signal in the dark ages*, *Mon. Not. Roy. Astron. Soc.* **508** (2021), no. 4 5709–5715, [[arXiv:2110.06447](#)].
- [84] Y. Yang, *Impact of radiation from primordial black holes on the 21-cm angular-power spectrum in the dark ages*, *Phys. Rev. D* **106** (2022), no. 12 123508, [[arXiv:2209.00851](#)].
- [85] G.-W. Yuan, L. Lei, Y.-Z. Wang, B. Wang, Y.-Y. Wang, C. Chen, Z.-Q. Shen, Y.-F. Cai, and Y.-Z. Fan, *Rapidly growing primordial black holes as seeds of the massive high-redshift JWST Galaxies*, *Sci. China Phys. Mech. Astron.* **67** (2024), no. 10 109512, [[arXiv:2303.09391](#)].
- [86] Z. Zhang, B. Yue, Y. Xu, Y.-Z. Ma, X. Chen, and M. Liu, *Cosmic radio background from primordial black holes at cosmic dawn*, *Phys. Rev. D* **107** (2023), no. 8 083013, [[arXiv:2303.06616](#)].
- [87] P. Jangra, D. Gaggero, B. J. Kavanagh, and J. M. Diego, *The cosmic history of Primordial Black Hole accretion and its uncertainties*, [arXiv:2412.11921](#).
- [88] A. Aguayo-Ortiz, E. Tejeda, O. Sarbach, and D. López-Cámara, *Spherical accretion: Bondi, Michel, and rotating black holes*, *Mon. Not. Roy. Astron. Soc.* **504** (2021), no. 4 5039–5053, [[arXiv:2102.12529](#)].
- [89] S. Das, M. R. Haque, J. Kalita, R. Karmakar, and D. Maity, *Impact of general relativistic accretion on primordial black holes*, [arXiv:2505.15419](#).
- [90] Y. Ali-Haïmoud and M. Kamionkowski, *Cosmic microwave background limits on accreting primordial black holes*, *Phys. Rev. D* **95** (2017), no. 4 043534, [[arXiv:1612.05644](#)].
- [91] J. H. MacGibbon and B. R. Webber, *Quark and gluon jet emission from primordial black holes:*

- The instantaneous spectra*, *Phys. Rev. D* **41** (1990) 3052–3079.
- [92] J. Auffinger, I. Masina, and G. Orlando, *Bounds on warm dark matter from Schwarzschild primordial black holes*, *Eur. Phys. J. Plus* **136** (2021), no. 2 261, [[arXiv:2012.09867](#)].
- [93] I. Masina, *Dark Matter and Dark Radiation from Evaporating Kerr Primordial Black Holes*, *Grav. Cosmol.* **27** (2021), no. 4 315–330, [[arXiv:2103.13825](#)].
- [94] **BICEP, Keck** Collaboration, P. A. R. Ade et al., *Improved Constraints on Primordial Gravitational Waves using Planck, WMAP, and BICEP/Keck Observations through the 2018 Observing Season*, *Phys. Rev. Lett.* **127** (2021), no. 15 151301, [[arXiv:2110.00483](#)].
- [95] Y. Mambrini, *Particles in the dark Universe*, Springer Ed., ISBN 978-3-030-78139-2 (2021).
- [96] S. Dodelson and M. S. Turner, *Nonequilibrium neutrino statistical mechanics in the expanding universe*, *Phys. Rev. D* **46** (1992) 3372–3387.
- [97] S. Hannestad and J. Madsen, *Neutrino decoupling in the early universe*, *Phys. Rev. D* **52** (1995) 1764–1769, [[astro-ph/9506015](#)].
- [98] A. D. Dolgov, S. H. Hansen, and D. V. Semikoz, *Nonequilibrium corrections to the spectra of massless neutrinos in the early universe*, *Nucl. Phys. B* **503** (1997) 426–444, [[hep-ph/9703315](#)].
- [99] G. Mangano, G. Miele, S. Pastor, T. Pinto, O. Pisanti, and P. D. Serpico, *Relic neutrino decoupling including flavor oscillations*, *Nucl. Phys. B* **729** (2005) 221–234, [[hep-ph/0506164](#)].
- [100] P. F. de Salas and S. Pastor, *Relic neutrino decoupling with flavour oscillations revisited*, *JCAP* **07** (2016) 051, [[arXiv:1606.06986](#)].
- [101] M. Escudero Abenza, *Precision early universe thermodynamics made simple: N_{eff} and neutrino decoupling in the Standard Model and beyond*, *JCAP* **05** (2020) 048, [[arXiv:2001.04466](#)].
- [102] K. Akita and M. Yamaguchi, *A precision calculation of relic neutrino decoupling*, *JCAP* **08** (2020) 012, [[arXiv:2005.07047](#)].
- [103] J. Froustey, C. Pitrou, and M. C. Volpe, *Neutrino decoupling including flavour oscillations and primordial nucleosynthesis*, *JCAP* **12** (2020) 015, [[arXiv:2008.01074](#)].
- [104] J. J. Bennett, G. Buldgen, P. F. De Salas, M. Drewes, S. Gariazzo, S. Pastor, and Y. Y. Y. Wong, *Towards a precision calculation of N_{eff} in the Standard Model II: Neutrino decoupling in the presence of flavour oscillations and finite-temperature QED*, *JCAP* **04** (2021) 073, [[arXiv:2012.02726](#)].
- [105] **Planck** Collaboration, Y. Akrami et al., *Planck 2018 results. X. Constraints on inflation*, *Astron. Astrophys.* **641** (2020) A10, [[arXiv:1807.06211](#)].
- [106] K. Abazajian et al., *CMB-S4 Science Case, Reference Design, and Project Plan*, [[arXiv:1907.04473](#)].
- [107] **CMB-HD** Collaboration, S. Aiola et al., *Snowmass2021 CMB-HD White Paper*, [[arXiv:2203.05728](#)].